1

# SU(2)-Yang-Mills thermodynamics and some implications

(SU(3) YMTD in passing)

[Utrecht, Sept. 18, 2006]

## Introduction

- failure of perturbative loop expansion of thermodynamical quantities:

small screening of magnetic sector

$\Rightarrow$ infrared instability, no convergence by simple power counting (Linde 1980, Polyakov 1978)

factorial growth of number of diagrams, no natural truncation at a finite order

( $\frac{\text{action of typical quantum fluctuation}}{\hbar}$ not guaranteed to be small )

$\Rightarrow$ expansion at best asymptotic (Dyson 1952, Hurst 1952, Thirring 1953, Peterman 1953)

- topological fluctuations may provide for mass-generating mechanism to evade infrared-catastrophe (Polyakov 1975)

(recall: in small-coupling expansion topological configurations entirely absent due to essential zero of $e^{-\frac{\text{const}}{g^2}}$ at $g=0$)

(2)

- <u>however</u>: microscopic analysis (semiclassical approx.) useless at large values of scale parameter ('t Hooft 1976)

- <u>thus</u>: consider only coarse-grained effects of interacting, radiatively modified topological defects

  $\Rightarrow$ inessential, highly complex microscopic physics averaged away
  <u>but</u> essential aspects (emergence of mass, dynamical gauge-symmetry breaking, maximal resolution scale) apparent

## Inert, adjoint scalar field at high temperatures

- in a given gauge (singular) $\exists$ absolutely stable (trivial holonomy), BPS saturated, top. configurations:

  for $|Q|=1$ $\rightarrow$ Harrington-Shepard (anti) calorons

- if an adjoint scalar $\phi = \phi^a \lambda^a$ emerges due to a spatial coarse-graining over noninteracting, classical config. [$\theta_{\mu\nu}[A] \equiv 0$]

  $\Rightarrow$ dimensionless phase $\hat{\phi}(\tau)$ periodic and classically determined, lies in kernel $\mathcal{K}$ of differential operator $\mathcal{D}$

- one can show that $\mathcal{K}$ defined by

$$(*)\quad \sum_{\substack{C,A\\(HS)}} \mathrm{tr} \int d\rho \int d^3x\, \lambda^a F_{\mu\nu}(\tau,\vec{0})\{(\tau,\vec{0}),(\tau,\vec{x})\} F_{\mu\nu}(\tau,\vec{x})\{(\tau,\vec{x}),(\tau,\vec{0})\}$$

(no contr. of higher n-point functions, only $|Q|=1$, <u>recall:</u> local def. trivial due to $F_{\mu\nu} = \pm \tilde{F}_{\mu\nu}$)

- <u>in evaluating $(*)$:</u>
  - only magnetic-magnetic correlation contributes
  - $\mathcal{D} = \partial_\tau^2 + \left(\frac{2\pi}{\beta}\right)^2$
  - BPS saturation of $\phi$ $\Rightarrow$ 'square-root' of $\mathcal{D}$ relevant

- assuming existence of a mass scale $\Lambda$ and analyticity in $\phi$ of RHS of BPS equation

$\rightarrow$ e.o.m. for $\phi$:

$$\boxed{\partial_\tau \phi = \pm \frac{2\pi i}{\beta} \lambda_3 \frac{\phi}{|\phi|^2} = \pm \frac{2\pi i}{\beta} \lambda_3 \phi^{-1}}$$

(global gauge choice)

$\Rightarrow (\;)^2$ RHS $\Rightarrow \boxed{V(|\phi|^2) = \frac{\Lambda^6}{|\phi|^2}}$ $\quad \left(\beta \equiv \frac{1}{T}\right)$

$$\Rightarrow \boxed{\phi(\tau) = \sqrt{\frac{\Lambda^3}{2\pi T}}\, \lambda_1 \exp\left[\mp \frac{2\pi i}{\beta} \lambda_3 \tau\right]}$$

decreasing relevance for large $T$

## (4) alternative derivation of $V(|\phi|^2)$:

consistency of Euler-Lagrange equation and BPS condition

$\Rightarrow$ (i) motion in a hyperplane in Lie-algeb. by gauge invariance of $V(|\phi|^2)$

(angular mom. conserved for central potential)

(ii) uniform angular motion

(iii) $$\frac{V(|\phi|^2)}{|\phi|^2} \stackrel{!}{=} -\frac{\partial V(|\phi|^2)}{\partial |\phi|^2}$$

$$\Rightarrow V(|\phi|^2) = \frac{\Lambda^6}{|\phi|^2}$$ (YM-scale $\Lambda$ as a constant of integration)

- coarse-graining procedure only viable if inertness of $\phi$ follows ($\exists\, \delta\phi \Rightarrow$ destabilization $\Rightarrow \phi$ useless)

action: $S_\phi = \mathrm{tr} \int \left( (\partial_\tau \phi)^2 + V(|\phi|^2) \right)$

$$\Rightarrow \boxed{M_\phi^2 = 2 \left. \frac{\partial^2 V}{\partial |\phi|^2} \right|_{|\phi| = \sqrt{\frac{\Lambda^3}{2\pi T}}} = 48\,\pi^2 T^2}$$

$$\Rightarrow \frac{M_\phi^2}{T^2} = 48\pi^2 \gg 1$$ (no statistical (on-shell) fluct.)

$$\Rightarrow \frac{M_\phi^2}{|\phi|^2} = 12\lambda^3 \gg 1 \quad \text{for } \lambda > 1,\ \lambda \equiv \frac{2\pi T}{\Lambda},$$

(no quantum fluctuations) but $\lambda \geq \lambda_c = 11.65$, later!

5

Question: Is the infinite-volume and scale-parameter average used to determine $\mathcal{D}$'s kernel $\mathcal{K}$ saturated at a finite cutoff $|\phi|^{-1}$?

$\lambda = \lambda_c$ we have

$$\left.\frac{|\phi|^{-1}}{\beta}\right|_{\lambda=\lambda_c} = 6.32$$

$\lambda > \lambda_c$ we have

$$\left.\frac{|\phi|^{-1}}{\beta}\right|_{\lambda>\lambda_c} = 6.32\left(\frac{\lambda}{\lambda_c}\right)^{3/2}$$

but:

Figure 1

$\Rightarrow$ $\mathcal{K}$ well saturated!

# Figure 1

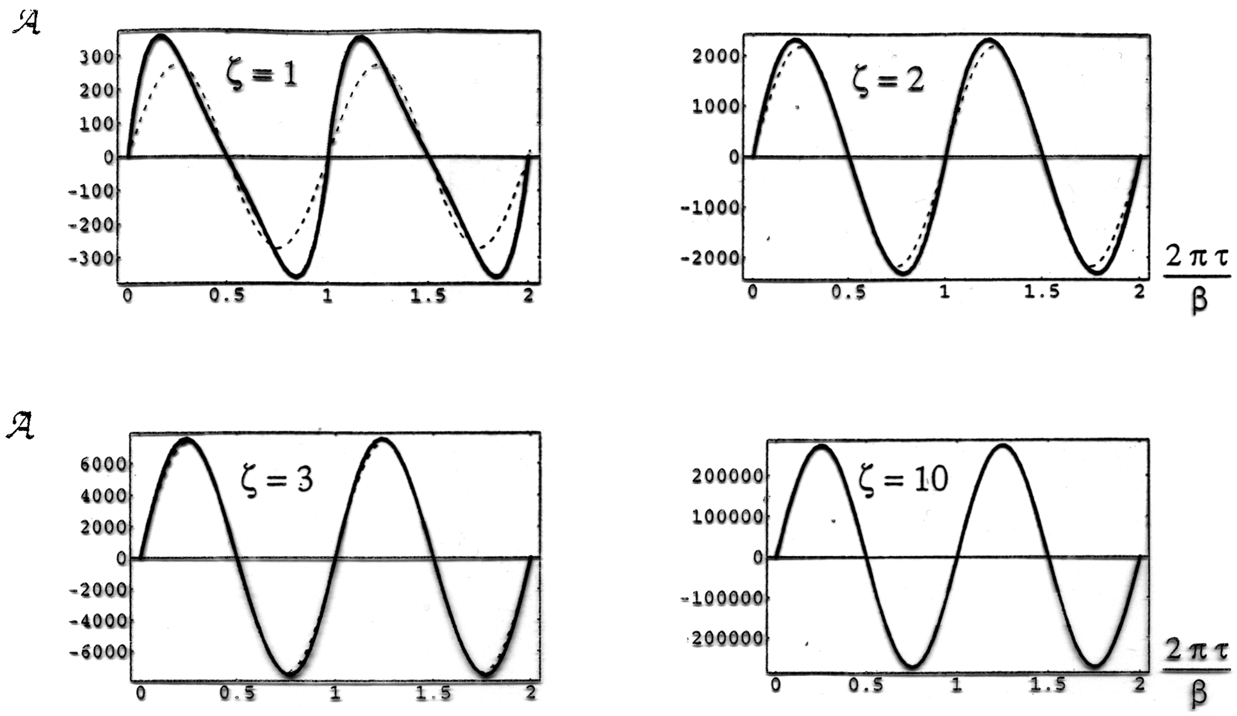


Figure 3.2: The function $\mathcal{A}(\frac{2\pi\tau}{\beta})$ plotted over two periods with different values of $\zeta$. For comparison the function $272\zeta^3 \sin(\frac{2\pi\tau}{\beta})$ is plotted as a dashed line. Already for $\zeta = 10$ the difference cannot be resolved any more.

| $\zeta$ | $\mathcal{A}(\frac{\pi}{2})/\zeta^3$ | $\zeta$ | $\mathcal{A}(\frac{\pi}{2})/\zeta^3$ | $\zeta$ | $\mathcal{A}(\frac{\pi}{2})/\zeta^3$ |
|---|---|---|---|---|---|
| | 301.295 | 10 | 272.776 | 100 | 272.026 |
| | 285.012 | 20 | 272.216 | 200 | 272.020 |
| | 278.828 | 30 | 272.107 | 300 | 272.018 |
| | 276.161 | 40 | 272.068 | 400 | 272.018 |
| | 274.794 | 50 | 272.050 | 500 | 272.018 |
| | | | | 1000 | 272.018 |

Table 3.1: Value of the function $\mathcal{A}$ at $\frac{\pi}{2}$ for several values of the cutoff $\zeta$. The cutoff dependence $\zeta^3$ has been divided out.

## Summary, field $\phi$:

selfconsistent spatial coarse-graining over stable, BPS saturated sector of SU(2) YMTD

$\Rightarrow$ inert, adjoint scalar $\phi$ such that coarse-graining sufficiently local to exclude configurations of topol. charge modulus $|Q|>1$, $\phi$'s potential unique (no shift $V(|\phi|^2) \to V(|\phi|^2) + \text{const}$)

## Fluctuations with $Q=0$

perturbative renormalizibility

$\Rightarrow$ form-invariance of $Q=0$-part of action under coarse-graining, gauge-invariance of effective action

$$\Rightarrow \quad \partial_\tau \phi \longrightarrow D_\mu \phi = \partial_\mu \phi - ie[a_\mu, \phi]$$

effective gauge coupling

$\Longrightarrow$ full effective action:

$$\boxed{S[a_\mu] = \mathrm{tr} \int \left( \frac{1}{2} G_{\mu\nu}^2 + (D_\mu \phi)^2 + V(|\phi|^2) \right)}$$

where $\phi$ is background field for dynamics of $a_\mu$.

$\Rightarrow$ e.o.m.

$$\boxed{D_\mu G_{\mu\nu} = -ie [\phi, D_\nu \phi]}$$

(7)

<u>solution:</u> $a_\mu^{gs} = \mp \delta_{\mu 4} \frac{2\pi}{\beta} \frac{\lambda_3}{2}$ (pure gauge)

$\Rightarrow$ $D_\mu \phi = 0$ , $G_{\mu\nu} = 0$

$\Rightarrow$ ground-state pressure and energy density

$\Rightarrow$ $\boxed{P^{gs} = -4\pi \Lambda^3 T = -\rho^{gs}}$

T-dependent cosmological constant

[ gluon exchanges, which do not propagate further then $|\phi|^{-1}$, are described by $a_\mu^{gs}$ after spatial coarse-graining; YM-scale $\Lambda$ (gravitationally) detectable ]

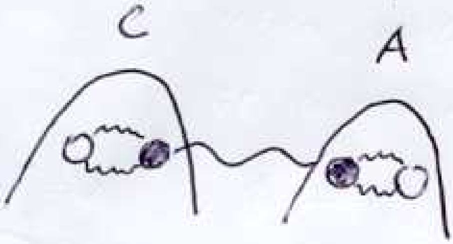


small holonomy

$\Rightarrow$ attraction between const. M-A, $P \sim 1$

large holonomy

$\Rightarrow$ repulsion between const. M-A, $P \sim e^{-40}$

(Diakonov et al, 2004)

$\Rightarrow$ negative ground-state pressure

(8) <u>rotation to unitary gauge:</u>

physical gauge needed to implement UV cutoff $|\phi|$ meaningfully

$$\phi = |\phi| \lambda_3 \, , \; a_\mu^{gs} = 0$$

(periodic but singular) gauge trafo: $\Omega(\tau) = \bar{\Omega}(\tau)\, Z(\tau)\, \Omega_{gl}$.

where
$$\bar{\Omega}(\tau) = \exp[\mp \pi \tfrac{\tau}{\beta} \lambda_3]$$
$$Z(\tau) = (2\theta(\tau - \tfrac{\beta}{2}) - 1)\, \mathbb{1}_2$$
$$\Omega_{gl} = \exp[-i \tfrac{\pi}{4} \lambda_2]$$

( periodicity of fluctuation $\delta a_\mu$ untouched under $\Omega(\tau) \Rightarrow \Omega(\tau)$ admissible )

<u>However:</u>
$$\mathbb{P}[a_\mu^{gs}] = -\mathbb{1}_2 \xrightarrow{\Omega} \mathbb{P}[a_\mu^{gs} = 0] = +\mathbb{1}_2$$
$SU(2) \to U(1)$

$\Longrightarrow \langle \mathbb{P} \rangle$ $Z_{2,\text{electric}}$ - degenerate

$\Longrightarrow$ $\boxed{\text{considered phase deconfining.}}$

fix $U(1)$-freedom by Coulomb-condition:
$$\partial_i \delta a_i = 0$$

$\Longrightarrow$ totally fixed, physical gauge.

<u>mass spectrum:</u>
$$m_1^2 = m_2^2 = 4e^2 |\phi|^2 \qquad (TLH)$$
$$m_3 = 0 \qquad (TLM)$$

(9)

# How does e depend on T?

real-time treatment:

propagator = quantum part + thermal (on-shell) part

in 1-loop expressions:

quantum part safely negligible due to maximal resolution $|\phi|$.

1-loop pressure:

$$P = P_{TLM} + 2P_{TLH} + P^{gs}$$

where: $$P_{TLH} = -6\int_0^\infty \frac{dk\,k^2}{2\pi^2}\ln\left(1-e^{-\frac{\sqrt{m_1^2+k^2}}{T}}\right)$$

$$P_{TLM} = \frac{\pi^2}{45}T^4,\quad P^{gs} = -4\pi\Lambda^3 T$$

now: invariance of Legendre-trafo

$$\rho = T\frac{dP}{dT} - P$$

$$\Rightarrow \quad \partial_m P = 0$$

$$\Rightarrow \quad \boxed{\partial_a \lambda = -\frac{24\lambda^4}{(2\pi)^6}\,a\,D(a)}$$

where: $\lambda = \frac{2\pi T}{\Lambda}$, $a = \frac{m_1}{2T}$, $D(a) = \int_0^\infty dx\,\frac{x^2}{\sqrt{x^2+a^2}}\,\frac{1}{e^{\sqrt{x^2+a^2}}-1}$

fixed points:

$a = 0$ (no detection of $SU(2) \to U(1)$ in spectrum)

$a = \infty$ (critical temperature $\lambda_c$)

▶ Figure 2

▶ Figure 3

Higher orders in the loop-expansion

in unitary-Coulomb gauge:

(i) off-shellness of propagating modes smaller than $|\phi|^2$

(ii) effective vertices not resolved

$\Rightarrow$ momentum transfers in effect. theory not larger than $|\phi|^2$

$\Rightarrow$ (i) $\Leftrightarrow$ $|p^2 - m_1^2| \leq |\phi|^2$ (TLH)

$|p^2| \leq |\phi|^2$ (TLM)

(ii) $\Leftrightarrow$ 4-vertex

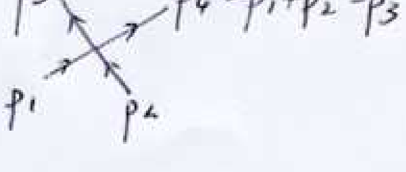

# Figure 2

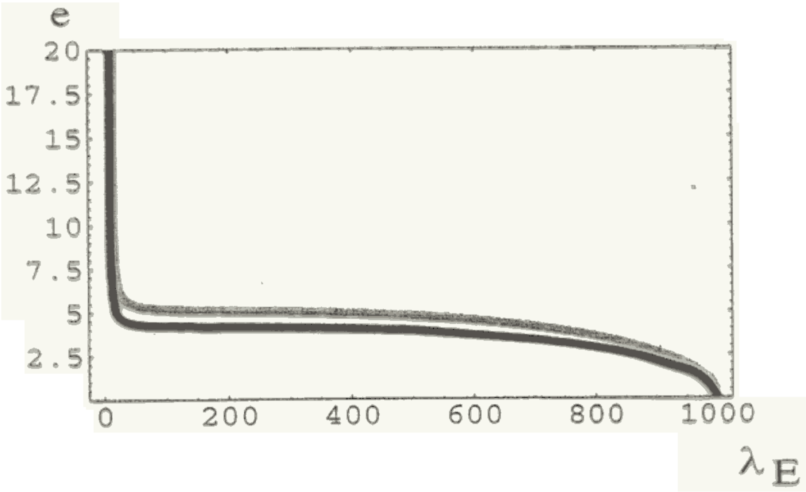


Figure 1: The temperature evolution of the gauge coupling $e$ in the electric phas
for SU(2) (grey line) and SU(3) (black line). The gauge coupling diverges logarith
mically, $e \propto -\log(\lambda_E - \lambda_{c,E})$, at $\lambda_{c,E} = 11.645$ (SU(2)) and $\lambda_{c,E} = 8.074$ SU(3
where $\lambda_E \equiv \frac{2\pi T}{\Lambda_E}$. The respective plateau values are $e = 5.14$ and $e = 4.17$.

magnetic charge of isolated, screened, and nonrelativistic monopoles ($g = \frac{4\pi}{e}$ for a single monopole) inside the spatial volume of typical size $|\phi|^{-3}$, and the behavio $e \sim -\log(T - T_{c,E})$ signals the vicinity of a phase transition where coarse-graine off-Cartan modes decouple and isolated magnetic monopoles become massless an thus condense.

# Figure 3

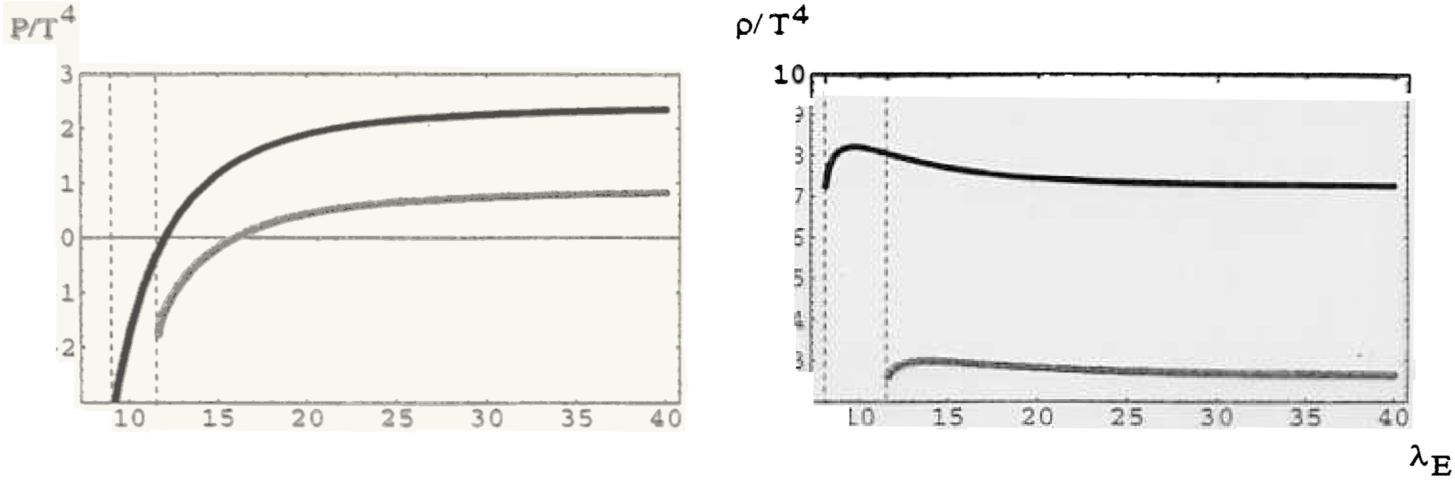


Figure 2: The ratios of energy density $\rho$ and pressure $P$ with $T^4$ for SU(2) (grey lines) and SU(3) (black lines). The vertical, dashed lines indicate the critical temperature for the onset of magnetic monopole condensation.

(11) $|(p_1+p_2)^2| \le |\Phi|^2$ (s-ch.)

$|(p_3-p_1)^2| \le |\Phi|^2$ (t-ch.)

$|(p_2-p_3)^2| \le |\Phi|^2$ (u-ch.)

- assuming that 1PI insertions into connected bubble diagrams are resummed (no pinch-singularities) estimate ratio of numb. $\tilde{K}$ of indep. radial loop-momenta (0-comp & mod. of spatial part) to numb. $K$ of independent constraints (Euler characteristic)

(A) 4-vertices only: ($V_4$-many)

$$\boxed{\frac{\tilde{K}}{K} \le \frac{4}{7}(1+V_4)}$$

($V_4 \geqslant 2$) (most constrained case)

(B) 3-vertices only: ($V_3$-many)

$$\boxed{\frac{\tilde{K}}{K} = \frac{2}{3}\left(1+\frac{2}{V_3}\right)}$$

($V_3 \geqslant 2$) (least constrained case)

(A) & (B) $\Longrightarrow$

$$\boxed{\frac{3}{4}\tilde{K} \geqslant \kappa \geqslant \frac{1}{2}\tilde{K}} \qquad (\tilde{K} \gg 1)$$

Where $\kappa$ is numb. constraints not used up at $\frac{\tilde{K}}{K} = 1$.

$\Longrightarrow$ Modulo 1PI resummations numb. connect. bubble diagrams most probably FINITE.

<u>In practice, one has:</u>

- Figure 4
  (2-loop corr. to pressure)

- Figure 5
  (TLM screening function)

postulating that $SU(2)_{CMB} \stackrel{\text{today}}{=} U(1)_Y$:

$\Longrightarrow \Lambda_{CMB} \sim 10^{-4}\,eV$

$\Longrightarrow$ modified black-body spectrum at $T =$ few times $T_{CMB}$ and $|\vec{p}| \lesssim 0.1\,T$

- Figures 6 & 7

# Figure 4

- dom. 2-loop contr. to pressure

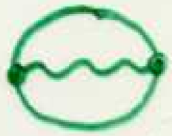

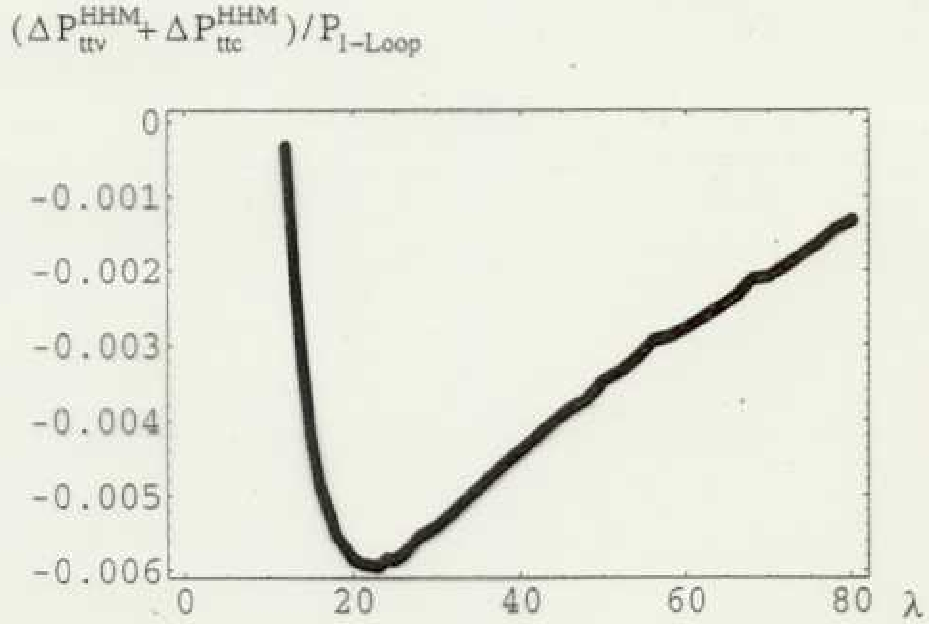


Figure 15: $\frac{\Delta P^{HHM}_{ttv} + \Delta P^{HHM}_{ttc}}{P_{\text{1-loop}}}$ as a function of $\lambda$.

# Figure 5

- TLM screening function from 1-loop polariz. tensor

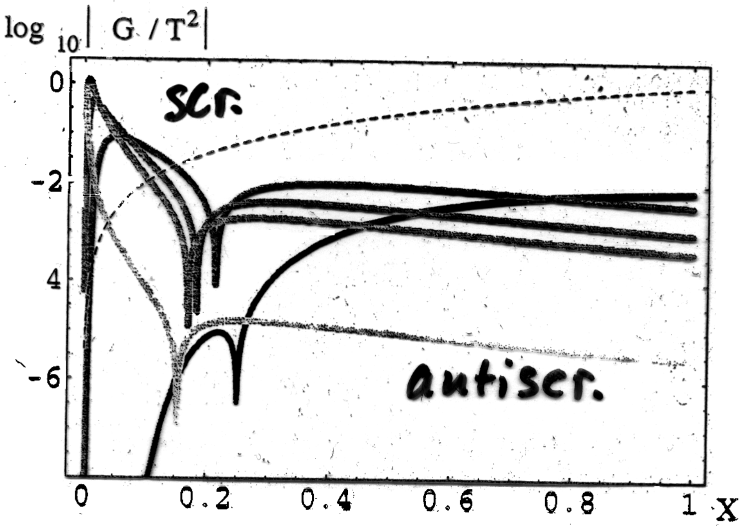


Figure 6: $\left|\frac{G}{T^2}\right|$ as a function of $X \equiv \frac{|\mathbf{p}|}{T}$ for $\lambda = 13$ (black), $\lambda = 2\,\lambda_{c,E}$ (dark grey), $\lambda = 3\,\lambda_{c,E}$ (grey), $\lambda = 4\,\lambda_{c,E}$ (light grey), $\lambda = 20\,\lambda_{c,E}$ (very light grey). The dashed curve is a plot of the function $f(X) = 2\log_{10} X$. TLM modes are strongly screened at $X$-values for which $\log_{10}\left|\frac{G}{T^2}\right| > f(X)$ ($\frac{\sqrt{G}}{T} > X$), that is, to the left of the dashed line.

$$p_0^2 = \vec{p}^{\,2} + G(p,T)$$

↳ setting $p^2 = 0$

# Figure 7

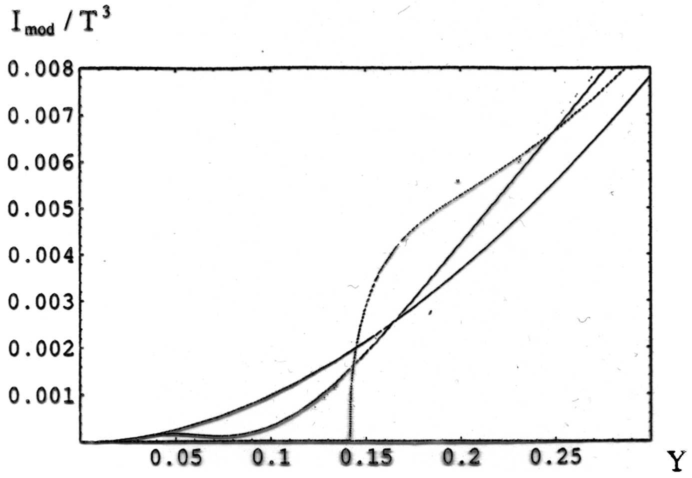


Figure 2: Dimensionless black-body spectral power $\frac{I_{mod}}{T^3}$ over dimensionless frequency $Y = \frac{\omega}{T}$ for $T = 3.85\,K$ (blue),$T = 4\,K$ (green),$T = 4.5$ (yellow), and $T = 6\,K$(red). The black curve is the curve of the unmodified spectrum.

# implications of $SU(2)_{CMB} \overset{\text{today}}{=} U(1)_Y$ ?

(Weinberg angle dynamical,
$U(1)_Y$ describes photon-PROPAGATION)

- missing spectral power at low $\ell$ in $\delta T \delta T$ angular correlation in CMB due to screening of correlating photons
- dynamical contrib. to CMB dipole
- PVLAS:

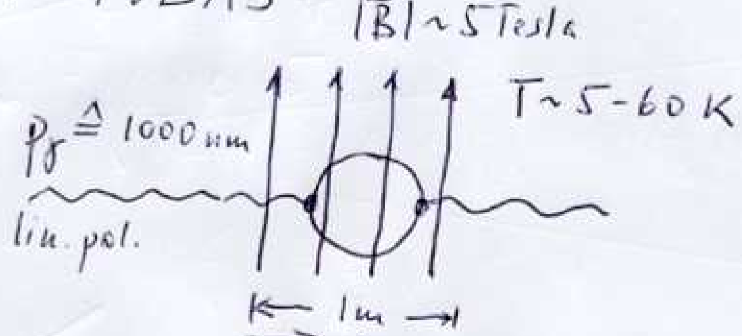


$\Rightarrow$ dynamically induced rotation of polariz. axis

# (14) precoufining & coufining phases, briefly:

## precoufining phase

- derivation of phase of complex scalar

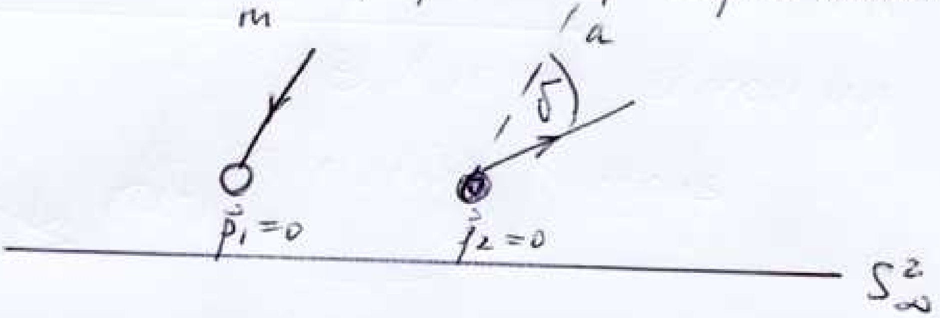


average magnetic flux through $S^2_\infty$ for $\vec{p}_{total} = \vec{p}_1 + \vec{p}_2 = 0 + 0 = 0$, $e \uparrow \infty$ $\left(g = \frac{4\pi}{e} \downarrow 0\right)$:

$$F_{\pm, th}(\delta) = \pm \frac{8\pi\delta}{e} \int d^3p \, \frac{\delta^{(3)}(\vec{p})}{\exp\left[\beta\sqrt{M^2_{mon} + \vec{p}^2}\right] - 1}$$

$$= \pm \frac{8\pi\delta}{e} \, \frac{e}{8\pi^2} \, \frac{1}{1 + \frac{1}{2}\frac{8\pi^2}{e} + \frac{1}{6}\left(\frac{8\pi^2}{e}\right)^2 + \dots}$$

$$\Rightarrow \boxed{\lim_{e \uparrow \infty} F_{\pm, th} = \pm \frac{\delta}{\pi} \qquad (0 \le \delta \le \pi)}$$

$$\Rightarrow \pm\frac{\delta}{\pi} \equiv \pm\frac{\tau}{\beta}$$

argument of periodic function $\hat{\varphi}$ with period unity.

$$\Rightarrow \mathcal{D} = \partial_\tau^2 + \left(\frac{2\pi}{\beta}\right)^2$$

BPS saturation (monopoles massless and at rest!) + $\Lambda$' (analyticity):

$$\Rightarrow \partial_\tau \varphi = \pm i \Lambda^3 \frac{\varphi}{|\varphi|^2} = \pm i \frac{\Lambda^3}{\bar{\varphi}}$$

15

$$\Rightarrow \boxed{\varphi = \sqrt{\frac{\Lambda^3}{2\pi T}} \exp\left[\pm 2\pi i \frac{\tau}{\beta}\right]}$$

$$\Rightarrow \quad S_\varphi = \int \left( \partial_\tau \bar{\varphi}\, \partial_\tau \varphi + V(|\varphi|^2) \right)$$

where $V(|\varphi|^2) = \frac{\Lambda'^6}{\bar{\varphi}\varphi}$

<u>$\varphi$ is inert:</u>

$$\frac{\partial^2_{|\varphi|} V(|\varphi|^2)}{|\varphi|^2} = 6\lambda'^3 \gg 1 \qquad \frac{\partial^2_{|\varphi|} V(|\varphi|^2)}{T^2} = 24\pi^2 \gg 1$$

where $\lambda' = \frac{2\pi T}{\Lambda'} \geq \lambda'_c = 7.34$ (later!)

<u>dual fluctuations with $Q=0$:</u>

$$S = \int \left( \frac{1}{4} G'^2_{\mu\nu} + \frac{1}{2} \overline{D'_\mu \varphi}\, D'_\mu \varphi + \frac{1}{2} \frac{\Lambda'^6}{\bar{\varphi}\varphi} \right)$$

where $G'_{\mu\nu} = \partial_\mu a'_\nu - \partial_\nu a'_\mu$ (dual gauge field)

$D'_\mu \varphi = \partial_\mu + ig a'_\mu$

<u>e.o.m.:</u> $\partial_\mu G'_{\mu\nu} = ig \left[ \overline{D'_\nu \varphi}\varphi - \bar{\varphi} D'_\nu \varphi \right]$

<u>solution:</u> $a'^{gs}_\mu = \pm \delta_{\mu 4} \frac{2\pi}{g\beta}$

$$\Rightarrow \boxed{P^{gs} = -\rho^{gs} = 2\pi \Lambda'^3 T}$$

[ dual fluctuations, which propagate no further than $|\varphi|^{-1}$ induce interactions between m & a thus shifting the ground-state energy density and pressure! ]

## Polyakov loop:

$$\mathcal{P} = \exp\left[ig \int_0^\beta d\tau\, a_4^{gs}\right] = 1$$

relation to unitary gauge:

$$\Omega = \exp\left[\pm 2\pi i \frac{\tau}{\beta}\right]$$

$$\Rightarrow \mathcal{P}[a_\mu^{gs}] = 1 \xrightarrow{\Omega} \mathcal{P}[a_\mu^{gs} = 0] = 1$$

$\Rightarrow$ ground state no longer $Z_{2,\text{electric}}$ degenerate!

## Spectrum:

$$m = g|\phi| = a'T \qquad (a' = 2\pi g \lambda'^{-3/2})$$

## invariance of Legendre trafo:

$$\Rightarrow \boxed{\partial_{a'} \lambda' = -\frac{12}{(2\pi)^6} \lambda'^4 a' D(a')}$$

$\Rightarrow$ evolution of $g$

▶ Figure 8

**remark:**
th. d. quantities 1-loop exact!

## How are $\Lambda$ and $\Lambda'$ related?

continuity of the pressure across the phase boundary:

$$\boxed{\Lambda = \left(\frac{1}{4}\right)^{1/3} \Lambda'}$$

# Figure 8

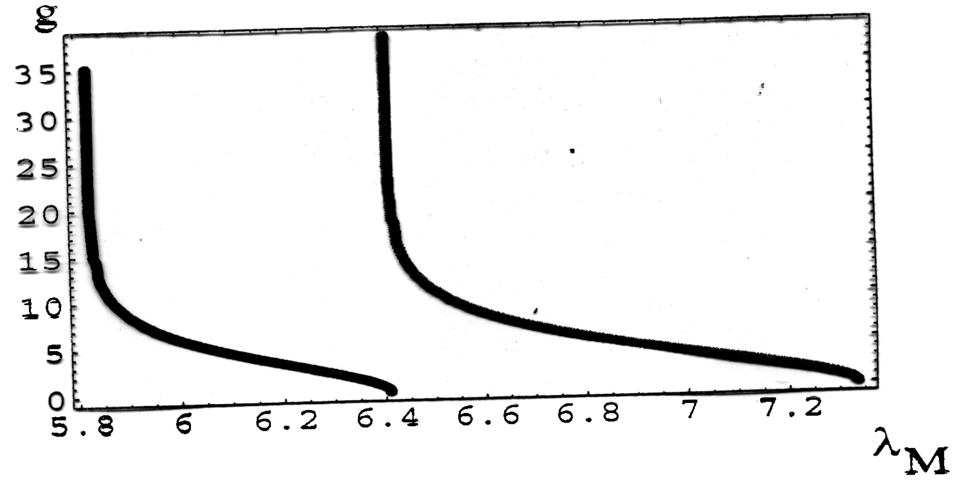


Fig. 17. The evolution of the effective gauge coupling $g$ in the magnetic phase for SU(2) (thick grey line) and SU(3) (thick black line). At $\lambda_{c,M} \equiv 6.41$ (SU(2)) and $\lambda_{c,M} \equiv 5.82$ (SU(3)) $g$ diverges logarithmically, $g \sim -\log(\lambda_M - \lambda_{c,M})$.

(17) <u>thermodynamical quantities:</u>

- Figure 9
- Figure 9'

pressure

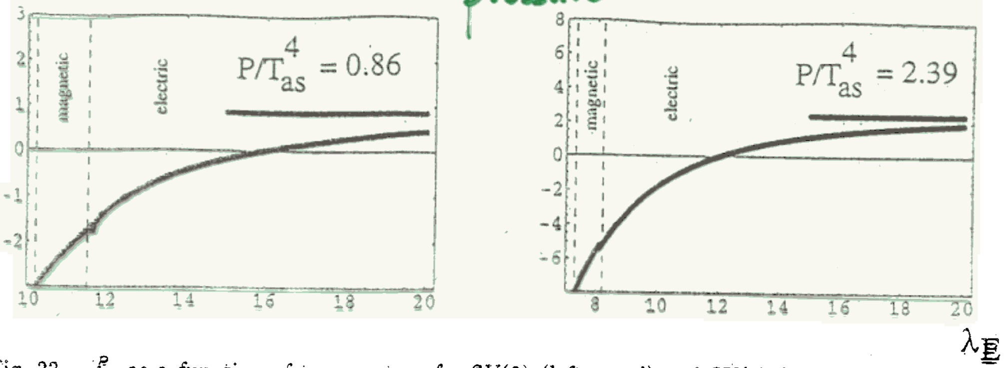


Fig. 22. $\frac{P}{T^4}$ as a function of temperature for SU(2) (left panel) and SU(3) (right panel). The horizontal lines indicate the respective asymptotic values, the dashed vertical lines are the phase boundaries.

energy density

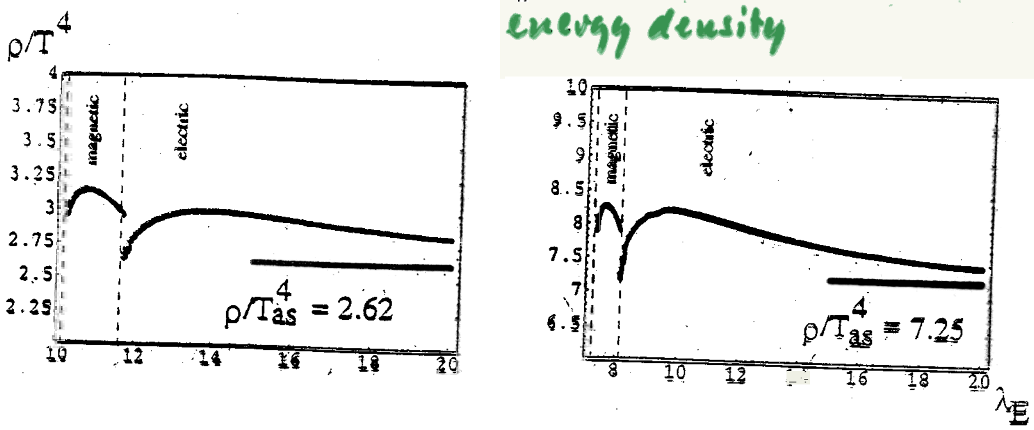


Figure 9

Fig. 24. $\frac{\rho}{T^4}$ as a function of temperature for SU(2) (left panel) and SU(3) (right panel). The horizontal lines indicate the respective asymptotic values, the dashed vertical lines are the phase boundaries.

entropy density

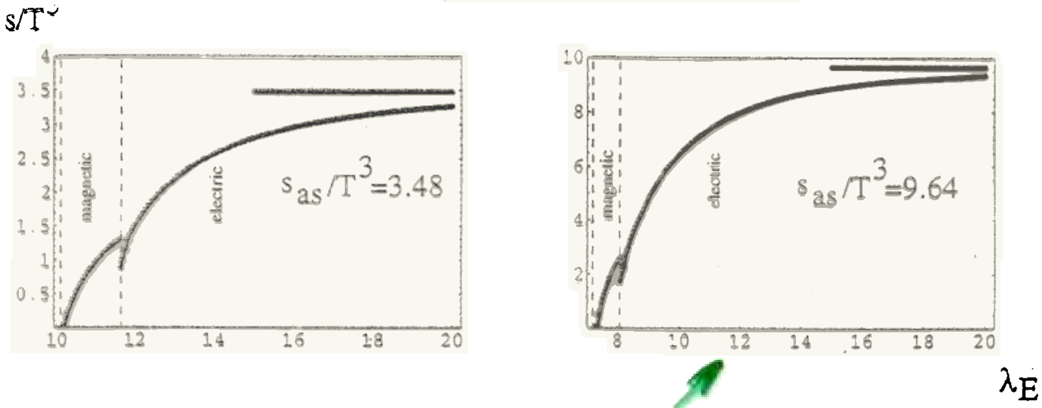


Fig. 31. $\frac{S}{T^3}$ as a function of temperature for SU(2) (left panel) and SU(3) (right panel). The horizontal lines signal the respective asymptotic values.

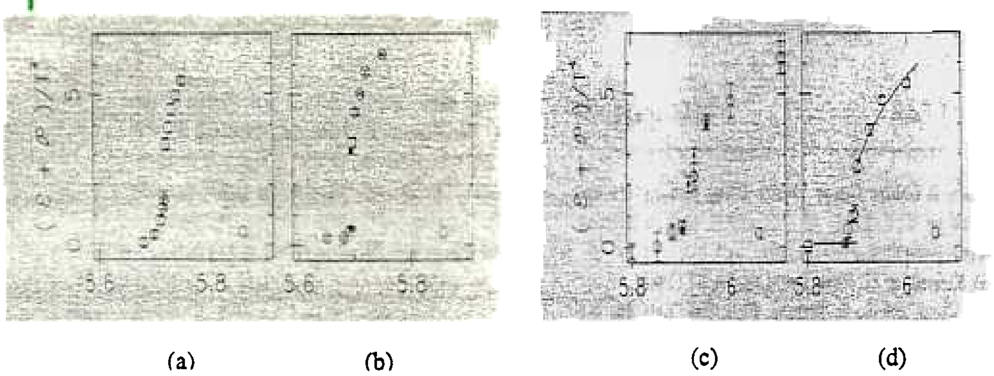


Fig. 32. $\frac{S}{T^3}$ as a function of $\beta$ obtained in SU(3) lattice gauge theory using the differential method and a perturbative beta function [76]. The simulations were performed on (a) $16^3 \times 4$, (b) $(24^3 \times 4)$-, (c) $(16^3 \times 6)$- (open circles) and $(20^3 \times 6)$- (closed circles), and (d) $(24^3 \times 6)$-lattices. Using the $(24^3 \times 6)$-lattice, the critical value of $\beta$ is between 5.8875 and 5.90.

Figure 9'

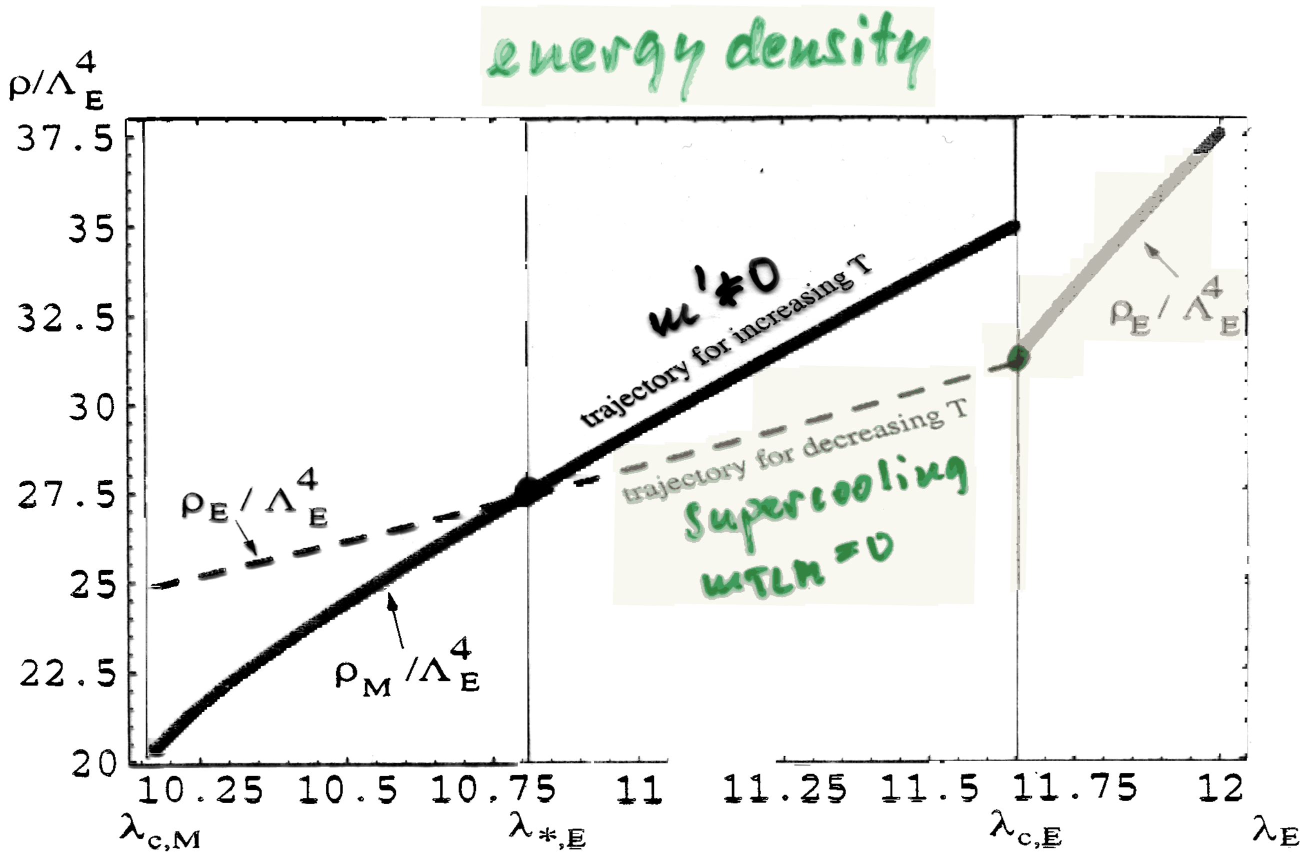


Figure 3: The situation for the (dimensionless) energy density in the critical regior the dashed line represents the continuation of the energy density of the deconfin ing phase (solid grey line) for $T < T_{c,E}$ (supercooled state, realized for decreasin temperature, $m_\gamma = 0$). The solid black line depicts the energy density in the precor fining phase (realized for increasing temperature, $m_\gamma > 0$). At the intersection poir $\lambda_E = \lambda_{*,E}$ a phase transition from the supercooled deconfining to the preconfinin dynamics occurs.

# Confining phase

microscopics:

- at $g<\infty$

  center-vortex loops, made of monopoles & antimonopoles flowing into opposite directions,

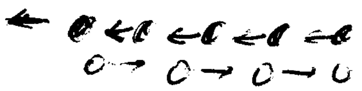

,

are instable (collapse)

- at $\lambda_c'$ they become massless and stable.

$\Rightarrow$ decay of the monopole condensate $\varphi$!

$\Rightarrow$ condensation of essentially noninteracting pairs of c, a.

- potential for vortex-loop condensate $\Phi$, Figure 10.

$$\boxed{V(\Phi)=\overline{\left(\frac{\Lambda''^3}{\Phi}-\Lambda''\Phi\right)}\left(\frac{\Lambda''^3}{\Phi}-\Lambda''\Phi\right)}$$

$$\left.\frac{\partial_\theta^2 V(\Phi)}{|\Phi|^2}\right|_{\Phi=\pm\Lambda''}=\left.\frac{\partial_{|\Phi|}^2 V(\Phi)}{|\Phi|^2}\right|_{\Phi=\pm\Lambda''}=8$$

(19) $\Rightarrow$ once $\bar{\Phi} = \pm \Lambda''$ reached $[\, V(\bar{\Phi} = \pm\Lambda'') = 0 \,]$

$\Rightarrow$ $\bar{\Phi}$ does not fluctuate

$\Rightarrow$ no more tunneling.

## Summary

- phase diagram of SU(2)/SU(3) YMTD

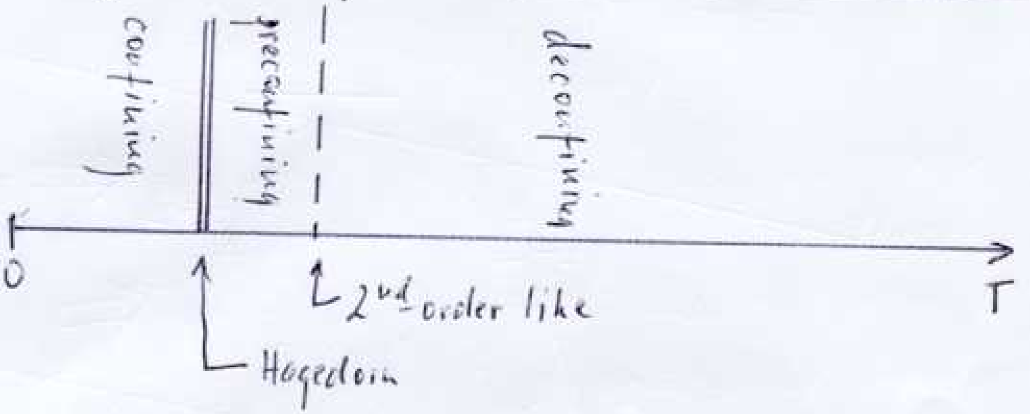


- Thank you for your attention!

# Figure 10

$V(\Phi)$

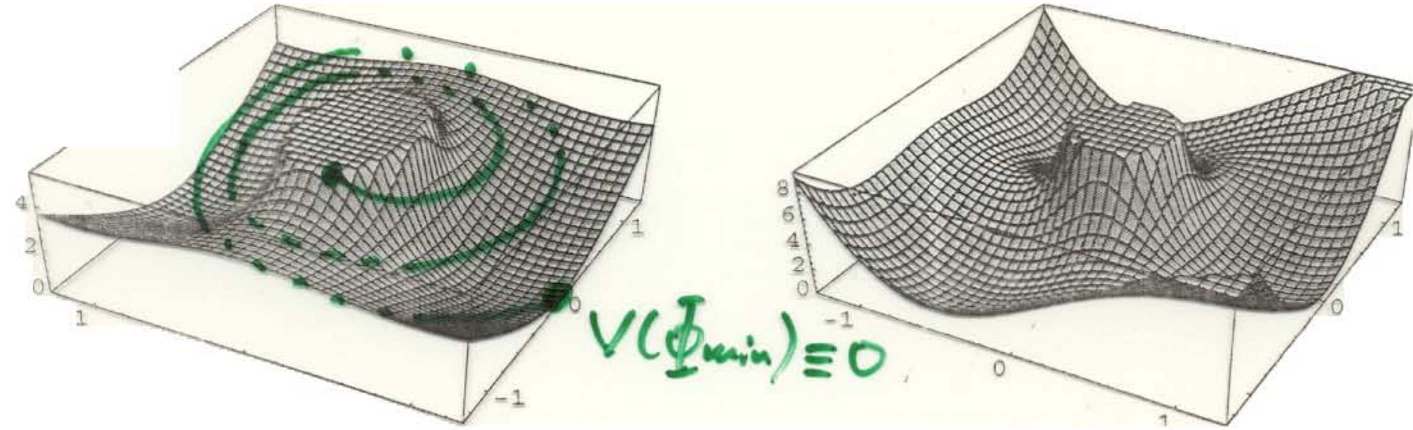


SU(2) SU(3)

## excitations

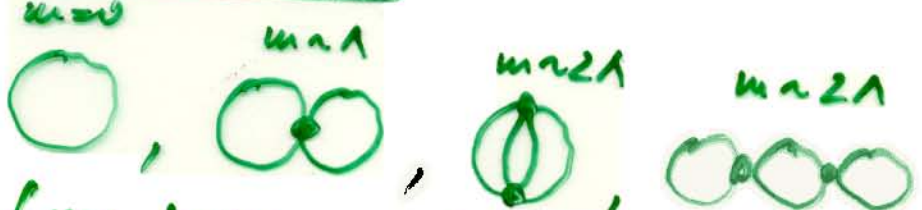


(vac bubbles in $\lambda\varrho^*$)

$\Rightarrow$ density of states $\varrho(E) > e^{\Lambda/T}$

$\rightarrow$ nonthermal Hagedorn transition